Preliminary communication / Communication

Iron, silicon, tin polymetallic complexes: formation of *trans, cis, cis*-[Fe(CO)$_2$(dppm-*P,P*)(SnClPh$_2$)$_2$] by silicon–tin exchange and its crystal structure

Pierre Braunstein [a],*, Chantal Charles [a], Richard D. Adams [b]

[a] *Laboratoire de chimie de coordination, UMR 7513 CNRS, université Louis-Pasteur, 4, rue Blaise-Pascal, 67070 Strasbourg cedex, France*
[b] *Department of Chemistry and Biochemistry, University of South Carolina, Columbia, SC 29208, USA*

Abstract

The reaction of the alkoxysilylcarbonylferrate [Fe(CO)$_3$(η^1-dppm){Si(OMe)$_3$}]$^-$ **1** (dppm = Ph$_2$PCH$_2$PPh$_2$) with [SnCl$_2$Ph$_2$] affords a Fe$_2$Si$_2$Sn chain complex **2** and a FeSn$_2$ complex **3** depending on the reaction conditions. Photochemical activation was found to trigger their transformation to another complex that has now been fully characterized by X-ray diffraction as *trans, cis, cis*-[Fe(CO)$_2$(dppm-*P,P*)(SnClPh$_2$)$_2$] **6**, which results from CO elimination and chelation of the dppm ligand. ***To cite this article: P. Braunstein et al., C.R. Chimie 8 (2005)***.

Résumé

La réaction de l'alcoxysilylcarbonylferrate [Fe(CO)$_3$(η^1-dppm){Si(OMe)$_3$}]$^-$ **1** (dppm = Ph$_2$PCH$_2$PPh$_2$) avec [SnCl$_2$Ph$_2$] conduit à un complexe en chaîne de cœur Fe$_2$Si$_2$Sn **2** et à un complexe FeSn$_2$ **3**, en fonction des conditions de réaction. Une activation photochimique favorise leur transformation en un nouveau complexe, qui a pu maintenant être complètement caractérisé par diffraction des rayons X comme étant le *trans, cis, cis*-[Fe(CO)$_2$(dppm-*P,P*)(SnClPh$_2$)$_2$] **6**, qui résulte de l'élimination de CO et de la chélation du ligand dppm. ***Pour citer cet article : P. Braunstein et al., C.R. Chimie 8 (2005)***.
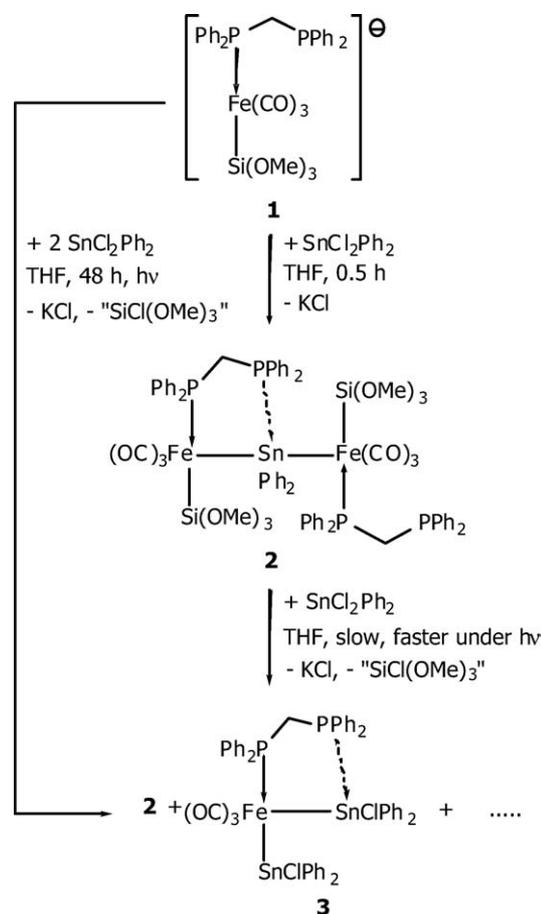
* Corresponding author.

E-mail address: braunst@chimie.u-strasbg.fr (P. Braunstein).

Although the study of molecular compounds containing a metal-silicon or metal-tin bond has been the subject of much research, this topic remains of considerable interest owing to its implications in various aspects of synthetic, structural and catalytic chemistry and for the formation of advanced materials [1–15]. Following the discovery that -Si(OR)$_3$ ligands can form a μ-η^2-Si–O bridge between two adjacent metals [16], which is thermodynamically stable but often displays hemilabile behaviour owing to the kinetic lability of the dative SiO→M bond, and then of an analogous behaviour for aminosilyl ligands [17], we explored the reactivity of the alkoxysilylcarbonylferrate *trans*-[Fe{Si(OMe)$_3$}(CO)$_3$(η^1-dppm)]$^-$
(dppm = Ph$_2$PCH$_2$PPh$_2$) (**1**) towards a range of transition and post-transition metal complexes susceptible to form such a Fe–Si–O→M moiety in order to study the scope of this phenomenon [2]. The presence of an assembling ligand such as dppm offers the possibility to increase the stability of the product by formation of a five-membered ring Fe(μ-dppm)M.

During our studies on the formation of mixed Fe-Si–Sn complexes, we noticed that the reactions of **1** with Sn(IV) precursors were very versatile and occurred with either retention of the silyl ligand or its exchange for a tin substituent. Thus, the reaction of K·**1** with [SnCl$_2$Ph$_2$] in THF, in a 1:1 ratio and under exclusion of light, led to the white product **2** in 89% yield (Scheme 1) [18].

When this reaction was performed with a 1:2 stoichiometry and for a longer period of time, a new complex was isolated, **3**, which contained two stannyl ligands, and another product was detected which could not be identified. It was shown that **2** is an intermediate in the synthesis of **3**. Its formation may be explained by the greater stability of the Fe–Sn bond compared to that of the Fe–Si bond [1,19]. The silyl ligand in **1** may thus be viewed as a protecting group of a second negative charge on the iron centre [20].

The X-ray structure analysis of **3** indicated no bonding interaction in the solid state between the 'dangling' PPh$_2$ group and the SnClPh$_2$ ligand cis to the P→Fe bond, their separation being 3.140(2) Å [18]. In solution, however, the presence in the ^{31}P{^{1}H} NMR spectrum of satellites for this resonance due to J(P^{117,119}Sn) couplings suggested the occurrence of a P→Sn interaction. It is noteworthy that when 2-(diphenylphosphino)pyridine was used as an assembling ligand, the


Scheme 1.

corresponding complex **4** clearly displayed a dative N→Sn bond (2.499(7) Å), consistent with the preference of the tin centre for a nitrogen over a phosphine donor [21].
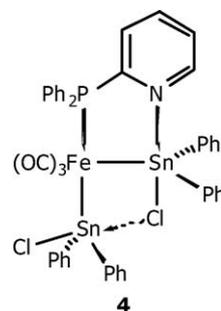

Whereas a complex analogous to **4** was obtained from [SnCl$_2$(*n*-Bu)$_2$], it is also important to remember that the nature of the anionic ligands on the Sn(IV) cen-

tre may exert a strong influence on the course of the reaction with the iron metalate and the structure of the product(s), as exemplified with the precursor [Sn(OAc)$_2$(*n*-Bu)$_2$] which reacted with **1** to afford **5** in 89% yield [22]. This complex was then used to prepare the first Fe-Pd-Sn cluster [23].
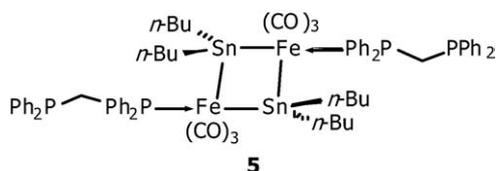
Since we noticed that in the presence of [SnCl$_2$Ph$_2$] and under photochemical activation, **2** progressively transforms into **3** and another product, we exposed a THF solution of pure **3** to sun or mercury lamp irradiation and obtained an almost quantitative spectroscopic (^{31}P{^{1}H} NMR) yield of this product, **6**. It is characterized by a ^{31}P{^{1}H} NMR singlet at δ 15.8, which suggests the formation of a symmetrical complex containing a chelating dppm ligand since the Fe-bound P donor in **3** resonates at δ 47.5 ppm.
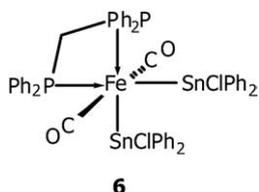
This has now been established by X-ray diffraction and Fig. 1 shows an ORTEP view of the structure of *trans, cis, cis*-[Fe(CO)$_2$(dppm-*P,P*)(SnClPh$_2$)$_2$] **6**. There are two, almost identical molecules in the unit cell and the bonding parameters for one of them are given in Table 1. Crystallographic data are presented in Table 2. The coordination geometry around Fe is octahedral, as expected for a Fe(II), d^6 centre. A slight distorsion results from the chelation of dppm, which imposes a P(1)–Fe–P(2) angle of 74.11(7)°. Consequently, the opposite angle Sn(1)–Fe–Sn(2) opens up to 94.04(4)°, which also reduces the steric hindrance between the SnClPh$_2$ ligands. The CO ligands are mutually trans, consistent with their ν(CO) absorptions at 2004w and 1934vs cm^{-1}. The other bonding parameters are con-
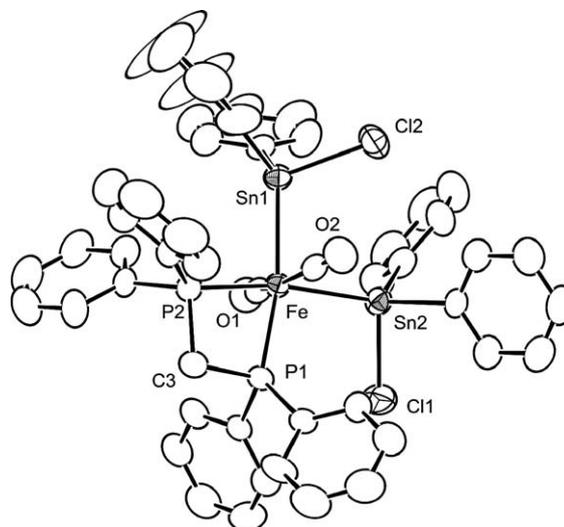
Fig. 1. View of the structure of *trans, cis, cis*-[Fe(CO)$_2$(dppm-*P,P*)(SnClPh$_2$)$_2$] **6**. Thermal ellipsoids are drawn at the 50% probability level.

Table 1
Selected Bond Distances (Å) and Angles (deg) in *trans, cis, cis*-[Fe(CO)$_2$(dppm-*P,P*)(SnClPh$_2$)$_2$] **6**

Fe–Sn (1)	2.566(1)	Sn(1)–C(4)	2.148(8)
Fe–Sn (2)	2.580(1)	Sn(1)–C(10)	2.165(7)
Fe–P(1)	2.262(2)	Sn(2)–Cl(1)	2.416(2)
Fe–P(2)	2.267(2)	Sn(2)–C(16)	2.152(7)
Fe–C(1)	1.796(9)	Sn(2)–C(22)	2.167(7)
Fe–C(2)	1.758(9)	C(1)–O(1)	1.144(8)
Sn(1)–Cl(2)	2.413(2)	C(2)–O(2)	1.169(8)
Sn(1)–Fe–Sn(2)	94.04(4)	P(2)–Fe–C(2)	96.1(2)
Sn(1)–Fe–P(1)	169.93(7)	C(1)–Fe–C(2)	162.0(3)
Sn(1)–Fe–P(2)	96.11(6)	Fe–Sn(1)–Cl(2)	108.46(6)
Sn(1)–Fe–C(1)	83.8(2)	Fe–Sn(1)–C(4)	120.9 (2)
Sn(1)–Fe–C(2)	85.4(2)	Fe–Sn(1)–C(10)	119.2(2)
Sn(2)–Fe–P(1)	95.72(6)	Fe–Sn(2)–Cl(1)	105.19(6)
Sn(2)–Fe–P(2)	169.84(7)	Fe–Sn(2)–C(16)	120.4(2)
Sn(2)–Fe–C(1)	81.2(2)	Fe–Sn(2)–C(22)	123.4(2)
Sn(2)–Fe–C(2)	85.3(2)	Fe–P(1)–C(3)	94.6(2)
P(1)–Fe–P(2)	74.11(7)	Fe–P(2)–C(3)	94.3(2)
P(1)–Fe–C(1)	95.3(2)	Fe–C(1)–O(1)	178.5(7)
P(1)–Fe–C(2)	97.8(2)	Fe–C(2)–O(2)	177.8(7)
P(2)–Fe–C(1)	99.3(2)	P1–C(3)–P(2)	96.0(3)

sistent with values found in related molecules. In view of the possibility for tin atoms to show different degrees of five-coordination [21,24,25], we examined the environment of the tin centres but found no unusual feature in their tetrahedral coordination. The Fe–Sn(1)–Cl(2) and Fe–Sn(2)–Cl(1) angles of 108.46(6) and 105.19(6)°,

Table 2

Summary of crystallographic data for the complex *trans, cis, cis*-[Fe(CO)$_2$(dppm-*P,P*) (SnClPh$_2$)$_2$] **6**

Formula	C$_{51}$H$_{42}$Cl$_2$FeO$_2$P$_2$Sn$_2$
Mol wt	1112.97
Cryst-system	monoclinic
Space group	*P*2$_1$/*a* (#14)
Radiation λ, Å	graphite-monochromated Mo Kα, λ = 0.71073
a, Å	19.071(4)
b, Å	13.309(5)
c, Å	20.848(5)
β, deg	115.77(2)
V, Å^3	4765(3)
Z	4
D$_{calcd}$, g cm^{-3}	1.55
μ, cm^{-1}	15.58 (Mo Kα)
2θ max, deg	40
No. obs. [*I* > 3 σ(*I*)]	3392
No. variables	542
R	0.03086
Rw	0.03069
Goodness of fit	1.67
Max/Min	0.999/0.801
Largest peak in final diff. map (e/Å^3)	0.4

respectively, are as expected and the intramolecular non-bonding Cl(2)⋯Sn(2) separation of 3.835(2) Å is significantly longer than in **4** (3.076(2) Å) [20]. Similarly, no Sn⋯Cl interaction was observed in the solid-state structure of the octahedral complex *cis*-[Fe(SnClMe$_2$)$_2$(CO)$_3$(PPh$_3$)] between the two *cis*-SnClMe$_2$ ligands [26].

In conclusion, we have now elucidated further the sequence of reactions leading from **2** to **3** and **6** and clearly established that upon photochemical activation of **3**, CO elimination and chelation of the dppm ligand represents the only reaction pathway observed. This complex **6** is the byproduct mentioned in Scheme 1 that had remained unidentified. We have also seen that the presence of two mutually *cis*-SnClR$_2$ ligands in an octahedral Fe(II) complex does not necessarily imply the occurrence of five-coordination around tin resulting from chloride bridge formation, although such situations have been clearly established in closely related complexes [21]. Obviously, rather subtle parameters influence the coordination geometry at tin, which also explains why solid-state and solution structures need not always to be identical.

1. Experimental Section

1.1. Synthesis

All experiments were carried out using Schlenk-tube techniques, under an atmosphere of oxygen-free nitrogen. Elemental C, H and N analyses were performed by the 'Service central de microanalyses du CNRS'. Infrared spectra were obtained using Perkin-Elmer 398 or Bruker IFS 66/113 (FTIR) spectrometers, and NMR spectra on a Bruker SY200 instrument with proton chemical shifts measured relative to tetramethylsilane and phosphorus chemical shifts relative to phosphoric acid (external reference) with downfield chemical shifts reported as positive. The reactions were generally monitored by IR in the ν(CO) region. The iron metalate *trans*-[Fe{Si(OMe)$_3$}(CO)$_3$(η^1-dppm)]$^-$ [27] and complexes **2** and **3** were prepared as described previously [18].

Two equivalents of solid [SnCl$_2$Ph$_2$] (0.688 g, 2.0 mmol) were added to a solution of K[Fe{Si(OMe)$_3$}(CO)$_3$(η^1-dppm)] at 0 °C prepared by reaction of KH with [HFe{Si(OMe)$_3$}(CO)$_3$(η^1-dppm)] (0.647 g, 1.0 mmol) in THF. The reaction mixture was stirred for 24 h near a UV lamp. The solution was filtered and fractional precipitation by progressive addition of hexane afforded first some white **2**. Slow diffusion of hexane into the filtrate afforded a mixture of **2** and of yellow **3** and finally **6** was obtained as orange crystals (85% yield). IR (THF): 2004w, 1934vs. ^{1}H NMR (CD$_2$Cl$_2$): δ 4.61 (t, 2H, PCH$_2$, ^2J(P–H) = 10.3 Hz), 6.98-7.95 (m, 20 H, Ph). ^{31}P{^{1}H} NMR (CD$_2$Cl$_2$): δ 15.8 (s, P(Fe), ^2J(P–^{117,119}Sn$_{cis}$) = 161 Hz, ^2J(P-^{117,119}Sn$_{trans}$) = 228 Hz.

1.2. Crystallographic analysis

Orange crystals of compound **6** suitable for X-ray diffraction were grown by slow diffusion of hexane into a solution in CH$_2$Cl$_2$ solvent mixture at –10 °C. The crystal used for data collection was mounted in a thin-walled glass capillary. Diffraction measurements were made on a Rigaku AFC6S fully automated four-circle diffractometer using graphite-monochromated Mo Kα radiation. The unit cell was determined and refined from 15 randomly selected reflections obtained by using the AFC6 automatic search, center, index, and least-squares routines. All structure solving calculations were

performed on a Digital Equipment Corp. VAXstation 3520 computer by using the TEXSAN program library (version 5.0) obtained from Molecular Structure Corp., Woodlands, TX. Neutral atom scattering factors were calculated by the standard procedures [28]. Anomalous dispersion corrections were applied to all nonhydrogen atoms [29]. Lorentz/polarization (Lp) and absorption corrections were applied to the data for the structure. Full-matrix least-squares refinements minimized the function: $\Sigma_{hkl} w \, (I \, F_\text{o} I - I \, F_\text{c} \, I)^2$, where $w = 1/\sigma(F_\text{o})^2$, $\sigma(F_\text{o}) = \sigma(F_\text{o}{}^2)/2 \, F_\text{o}$ and $\sigma(F_\text{o}{}^2) = [\sigma(I_\text{raw})^2 + (0.02 \, I_\text{net})^2]^{1/2}/Lp$. The structure was solved by a combination of direct methods (MITHRIL) and difference Fourier syntheses. All non-hydrogen atoms were refined with anisotropic thermal parameters. The positions of all hydrogen atoms were calculated by assuming idealized geometries with C–H = 0.95 Å. They were added to the structure factor calculations, but the positions were not refined. The crystal data and a summary of the analysis are given in Table 2. CCDC 239721 contains the supplementary crystallographic data for **6**. These data can be obtained free of charge via www.ccdc.cam.ac.uk/conts/retrieving.html (or from the Cambridge Crystallographic Data Centre, 12 Union Road, Cambridge CB21EZ, UK; fax: (+44)1223-336-033; or deposit@ccdc.cam.ac.uk).

Acknowledgements

References

[1] B.J. Aylett, Adv. Inorg. Chem. Radiochem. 25 (1981) 1.
[2] P. Braunstein, M. Knorr, C. Stern, Coord. Chem. Rev. 178-180 (1998) 903.
[3] P. Braunstein, X. Morise, Chem. Rev. 100 (2000) 3541.
[4] B. Marciniec, NATO Science Series, II: Mathematics, Physics and Chemistry 56 (2002) 391.
[5] B. Marciniec, H. Maciejewski, Coord. Chem. Rev. 223 (2001) 301.
[6] B. Marciniec, Appl. Organometal. Chem. 14 (2000) 527.
[7] M. Okazaki, S. Ohshitanai, M. Iwata, H. Tobita, H. Ogino, Coord. Chem. Rev. 226 (2002) 167.
[8] M. Okazaki, H. Tobita, H. Ogino, Dalton Trans. 493 (2003).
[9] M. Okazaki, E. Suzuki, N. Miyajima, H. Tobita, H. Ogino, Organometallics 22 (2003) 4633.
[10] H. Tobita, A. Matsuda, H. Hashimoto, K. Ueno, H. Ogino, Angew. Chem. Int. Ed. Engl. 43 (2004) 221.
[11] U. Burckhardt, G.L. Casty, J. Gavenonis, T.D. Tilley, Organometallics 21 (2002) 3108.
[12] B.V. Mork, T.D. Tilley, Angew. Chem. Int. Ed. Engl. 42 (2003) 357.
[13] M. Veith, Eur. J. Inorg. Chem. 9 (2000) 1883.
[14] M. Veith, Dalton Trans. 2405 (2002).
[15] A.G. Davies, Organotin Chemistry, Wiley-VCH, Weinheim, Germany, 2004.
[16] P. Braunstein, M. Knorr, A. Tiripicchio, M. Tiripicchio Camellini, Angew. Chem. Int. Ed. Engl. 28 (1989) 1361.
[17] P. Braunstein, C. Stern, C. Strohmann, N. Tong, Chem. Commun. (1996) 2237.
[18] P. Braunstein, M. Knorr, M. Strampfer, A. Decian, J. Fischer, J. Chem. Soc., Dalton Trans. (1994) 117.
[19] C.S. Cundy, B.M. Kingston, M.F. Lappert, Adv. Organomet. Chem. 11 (1973) 253.
[20] U. Schubert, in: N. Auner, J. Weis (Eds.), Organosilicon Chemistry, From Molecules to Materials, VCH, Weinheim, Germany, 1994 , p. 205.
[21] P. Braunstein, C. Charles, G. Kickelbick, U. Schubert, Chem. Commun. (1997) 1911.
[22] P. Braunstein, C. Charles, R.D. Adams, R. Layland, J. Cluster Sci. 7 (1996) 145.
[23] P. Braunstein, C. Charles, G. Kickelbick, U. Schubert, Chem. Commun. (1997) 2093.
[24] F.P. Boer, J.J. Flynn, H.H. Freedman, S.V. Mckinley, V.R. Sandel, J. Am. Chem. Soc. 89 (1967) 5068.
[25] M. Elder, W.A.G. Graham, D. Hall, R. Kummer, J. Am. Chem. Soc. 90 (1968) 2189.
[26] M. Knorr, H. Piana, S. Gilbert, U. Schubert, J. Organomet. Chem. 388 (1990) 327.
[27] P. Braunstein, M. Knorr, U. Schubert, M. Lanfranchi, A. Tiripicchio, J. Chem. Soc., Dalton Trans. (1991) 1507.
[28] International Tables for X-ray Crystallography, Kynoch Press, Birmingham, England, Vol., IV, 1975 , pp. 99–101 (Table 2.2B).
[29] in: International Tables for X-ray Crystallography, Kynoch Press, Birmingham, England, Vol., IV, 1975, pp. 149–150 (Table 2.3.1).